JOURNAL OF MATERIALS SCIENCE 27 (1992) 3963–3968

Microstructural changes of polycrystalline nickel during high-temperature deformation at ambient and high pressures

J. GROZA, S. MEAGHER, R. S. BORCH*, H. W. GREEN III*, A. K. MUKHERJEE
*Department of Mechanical, Aeronautical and Materials Science, and * Department of Geology, University of California, Davis, CA 95616, USA*

The microstructures of polycrystalline nickel, deformed in compression at temperatures of 1000–1500 K at high pressure (1500 MPa) and at ambient (0.1 MPa) pressure, were compared. Dynamic recrystallization and strain-induced grain growth were observed to occur during creep tests at both pressure levels. Our experimental results at ambient pressure are in good agreement with Sandstrom and Lagneborg's theory on dynamic recrystallization. However, high-pressure application considerably retarded recrystallization and grain-growth kinetics. This behaviour was attributed to an increase in the activation energy for grain-boundary migration at high pressure.

1. Introduction

The high-temperature mechanical behaviour of pure nickel at ambient pressure is well characterized. This was the primary reason for using nickel in order to clarify the understanding of the rate-controlling mechanism for creep over a large pressure range and to address a long-standing controversy on the activation energies and volumes for creep. The question whether the activation energy for high-temperature creep is stress dependent and higher than that for self-diffusion has been specifically addressed in a previous study [1]. In that study, by collecting creep data over a large range of temperatures and pressures, Meagher *et al.* have shown that the activation energy remains constant, is independent of stress, and is equal to the activation energy for self-diffusion. Poirier's argument on the discrepancy between activation energies for creep and self-diffusion [2, 3] has been answered by the alternative suggestion that the stress exponent, n, rather than the activation energy, varies with stress. An important result of the above study is that for low normalized stresses ($\sigma/G < 10^{-4}$), the "natural" stress exponent of $n = 3$ is approached. This result is consistent with recent studies on metals and ceramics and Weertman and Weertman's new model that proposes a "universal" power law creep with a basic stress-dependence of 3 [4].

An additional aim of the above study [1] of creep at high pressures was to compare the activation volume for creep with that for self diffusion. Furthermore, a careful comparison of microstructures between samples tested at high pressure and at 1 atm complemented the creep-test data. While measurement of the activation volume was beyond the resolution of high-pressure apparatus, novel microstructural characteristics have been revealed mainly in connection with pressure effects on microstructures. These aspects will constitute the subject of the present paper.

2. Experimental procedure

The material used in this investigation was Nickel 270. The as-received material of 99.98% nominal purity was 35% cold-worked. Compression creep specimens of two sizes (3 mm diameter and 7 mm high, and 13 mm diameter and 19 mm high) were used for high-pressure and ambient-pressure tests, respectively. Constant strain-rate tests were conducted at 1 atm in a MTS servo-hydraulic machine and at high pressure in a modified "Griggs" piston–cylinder apparatus. Constant strain-rate tests (10^{-5}–$10^{-3}\,s^{-1}$) in a molten salt environment between 1100 and 1550 K were performed in both cases. Details of the experimental apparatus are given in a previous paper [1].

In order to compare the results from the two types of tests, the heating rate to creep temperature ($100\,K\,h^{-1}$), testing environment (eutectic chloride mixture) and friction conditions at the specimen ends were kept the same for both equipments. A separate set of experiments with similar heating cycles at 1 atm and at high pressure were employed for detailed assessment of the effects on microstructure of both heating and cooling conditions and pressure on microstructure (Fig. 1). Specimens were routinely quenched from high temperature in the pressurized apparatus, whereas they were slowly cooled from the 1 atm apparatus. Only two specimens were quenched in the latter case. In addition, heating cycle experiments were conducted in both sets of apparatus but without deformation.

Specimens for optical microscopy were prepared using standard metallographic methods and etched

0022–2461

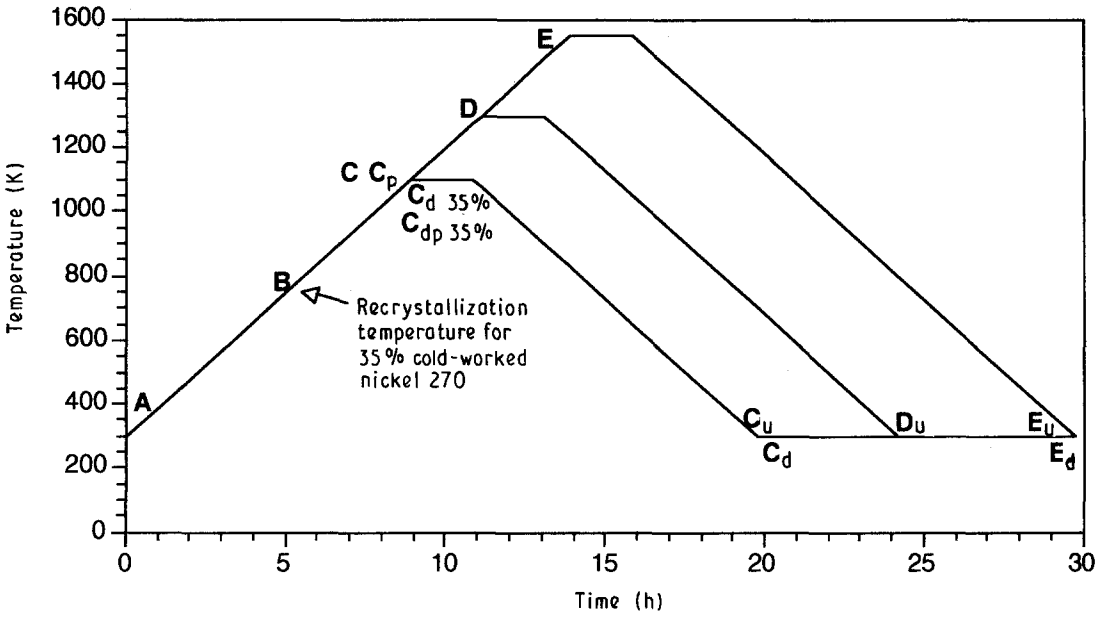

Figure 1 Schematic representation of heating cycles with and without deformation at ambient and high pressure. A, as received; B ramped to 750 K, air cooled; C, ramped up to 1100 K, air cooled; C_p, ramped to 1100 K at 1500 MPa, quenched; $C_{d35\%}$, ramped to 1100 K, deformed 35% at 0.1 MPa, $\dot{\varepsilon} = 10^{-4}\,s^{-1}$, ice quenched; $C_{dp35\%}$, same as $C_{d35\%}$ but at 1500 MPa; C_d, ramped to 1100 K, deformed 70% at 0.1 MPa, $\dot{\varepsilon} = 10^{-4}\,s^{-1}$, cooled under load at 100 K h^{-1}; C_u, ramped to 1100 K, maintained 2 h, cooled at 100 K h^{-1}; D, ramped to 1300 K, air cooled; D_u, same as C_u but at 1300 K; E, ramped up to 1550 K, air cooled; E_u, same as C_u, but at 1550 K; E_d, ramped to 1550 K, deformed 70%, $\dot{\varepsilon} = 10^{-4}\,s^{-1}$, cooled under load at 100 K h^{-1}.

with equal parts of nitric acid and distilled water. TEM specimens were cut parallel to the stress axis, mechanically thinned to less than 0.3 mm and finally thinned in an ethanol–20% perchloric acid solution using a dual-jet electro-polisher.

3. Results

Representative strain–stress curves for experiments conducted at 1 atm and high pressure are shown in Fig. 2. A common feature of the curves obtained at ambient pressure is the oscillation of flow stress especially during the early stages of deformation. The steady-state flow stress or fluctuating saturation stress varies in a consistent way with temperature and strain rate. Generally the oscillations are of about 3–4 MPa and increase with increasing temperature and decreasing strain rate. The oscillation does not depend on the initial grain size. In contrast, the peak stress values are more sensitive to grain size and grain-size distribution. If a critical strain, ε_{cr}, is measured at peak flow stress, it decreases when temperature increases. The oscillations at high pressure are less consistent and do not display the usual peak stress characteristic of the 1 atm experiments.

Grain-size measurements after various heating cycles at 1 atm and high pressure with and without deformation, are given in Table I. Representative optical microstructures are shown in Fig. 3. An interesting difference between 1 atm and high-pressure deformation microstructures is the much more irregular boundaries present after testing at high pressure (Fig. 3b). All specimens heated above 800 K are completely recrystallized.

As expected, recrystallization and grain growth occur during slow heating to 1100–1500 K prior to creep testing. For 1 atm experiments, grain-growth rate decreases appreciably starting at 1300 K. A 2 h holding time at temperature and a very slow cooling rate, compared to air cooling, has a minor influence on grain size. For example, grain size was about only 11% larger after an additional 2 h hold at 1100 K and slow cooling (Specimen C_u), compared to the air-cooled specimen, directly after heating to 1100 K (Specimen C).

Accurate calculations of activation energies for grain growth could not be performed due to variations of both time and temperature. However, an engineering-type compensation of heating rate to a corresponding fictitious temperature for the same annealing time enabled us to use the time law for grain growth of the form [5]

$$D = (at)^n \qquad (1)$$

where D is the grain size, t is time, $n = 0.5$ and a depends exponentially on temperature. Then, the calculated activation energy for isochronous grain growth is $\sim 45\,kJ\,mol^{-1}$. Although this energy is purely an estimated value, it is important to note that it is of the order of magnitude of the activation energy of nickel grain-boundary self-diffusion. It is also noteworthy that this result is in good qualitative agreement with similar values of activation energies for grain-boundary migration that were found in pure lead, tin and cadmium in the same normalized temperature range (above 0.7 T_m). Furthermore, the observed transition temperature for the onset of grain-boundary migration (1300 K) lies at about 0.75 T_m, which is consistent with the Haessner and Hoffman theory on the temperature dependence of grain-boundary migration in pure metals [5]. At high pressures, nickel was completely recrystallized during the heating cycle

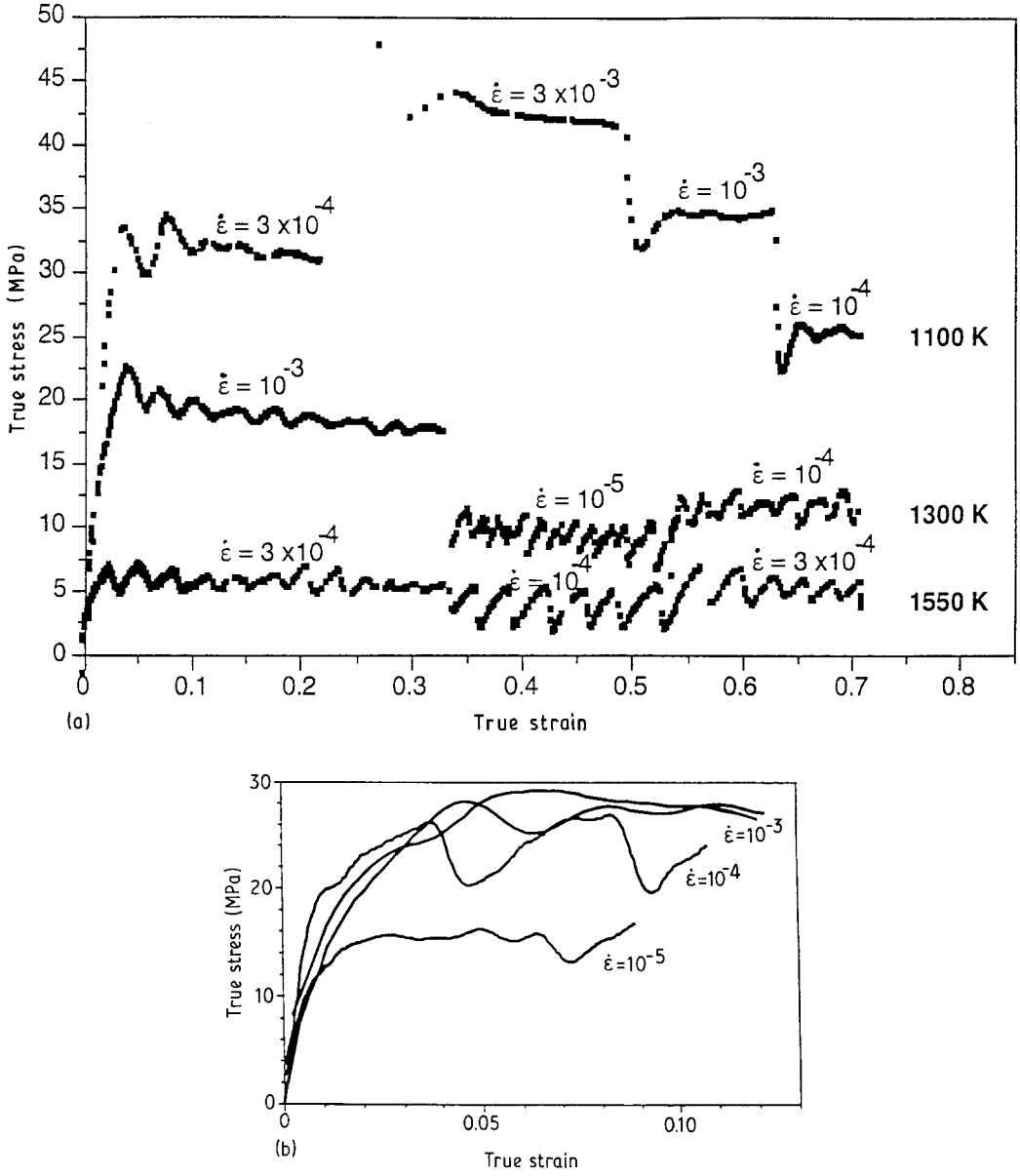

Figure 2 Representative stress–strain curves at (a) 0.1 and (b) 800 MPa. $T = 1300$ K. In 1 atm experiments the strain rate was stepped at various strain intervals.

TABLE I Grain-size measurements as a function of pressure and heating/cooling cycles

Sample[a]	Pressure (MPa)	Temp. (K)	Time at temp. (h)	Strain, (%)	Cooling rate ($K\,s^{-1}$)	Grain size (μm)
B	0.1	800	–	–	6	125 ± 16
C	0.1	1100	–	–	6	230 ± 33
C_p	1500	1100	–	–	125	142 ± 25
C_u	0.1	1100	2	–	0.025	257 ± 32
C_{d35}	0.1	1100	2	35	0.025	525 ± 72
C_{d70}	0.1	1100	2	70	0.025	1164 ± 220
C_{dp}	1500	1100	2	35	0.025	197 ± 17
D	0.1	1300	–	–	6	247 ± 32
D_u	0.1	1300	2	–	0.025	276 ± 46
E	0.1	1550	–	–	6	263 ± 34
E_u	0.1	1550	2	–	0.025	280 ± 31
E_d	0.1	1550	2	70	0.025	1625 ± 342

[a] For sample notation, see Fig. 1.

to 1100 K although the grain diameter was considerably finer than after a similar heating cycle under 1 atm pressure.

At ambient pressure, grain growth is considerably enhanced with strain, temperature, and initial grain size. Although strain-enhanced grain growth is observed during creep at high pressure, the kinetics of the process is considerably slower than at 1 atm. For

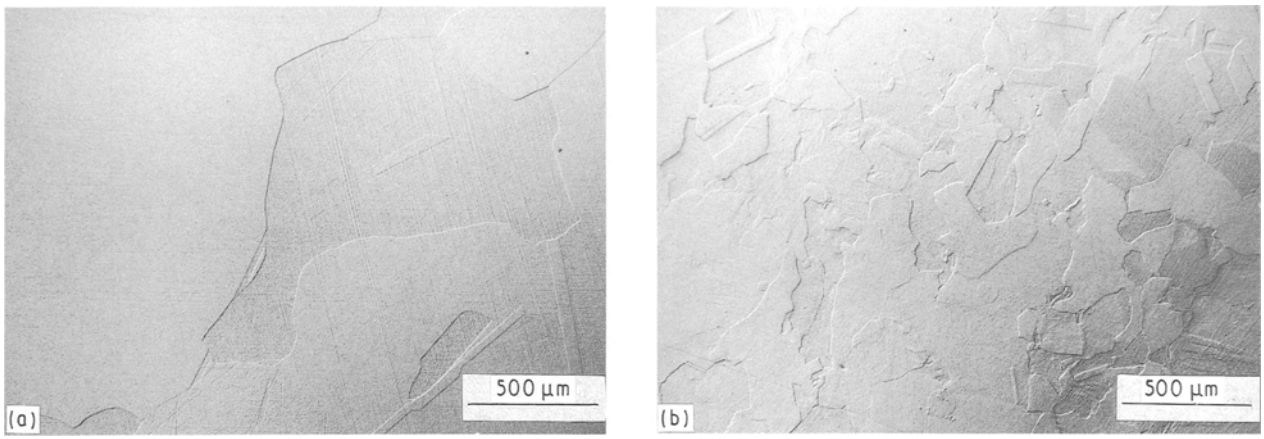

Figure 3 Recrystallized grains in nickel cycled to 1100 K and deformed 35% at (a) 0.1 and (b) 1500 MPa.

instance, at 1100 K the strain-enhanced grain growth was only 38% at 1500 MPa (Sample C_{dp}) compared to 125% at ambient pressure (Sample C_{d35}) for the same amount of strain.

Typical TEM structures of the as-received, statically recrystallized, and deformed nickel under 1 atm and high pressure are shown in Fig. 4. The as-received cold-worked material displays a cell structure with cell walls formed by irregular dislocation tangles and a low dislocation density in the cell interior (Fig. 4a). This structure is in agreement with the recovery mechanism maps of Parker *et al.* [6] and moderate value of stacking-fault energy in nickel which allows cross-slip to occur. The statically recrystallized material displays mainly dislocation-free grains (Fig. 4b).

The presence of a dislocation substructure within the recrystallized grains is a typical feature of nickel specimens after creep deformation at 0.1 and 1500 MPa (Fig. 4c–g). At both pressures, the dislocation structure is similar with diffuse cell walls and a range

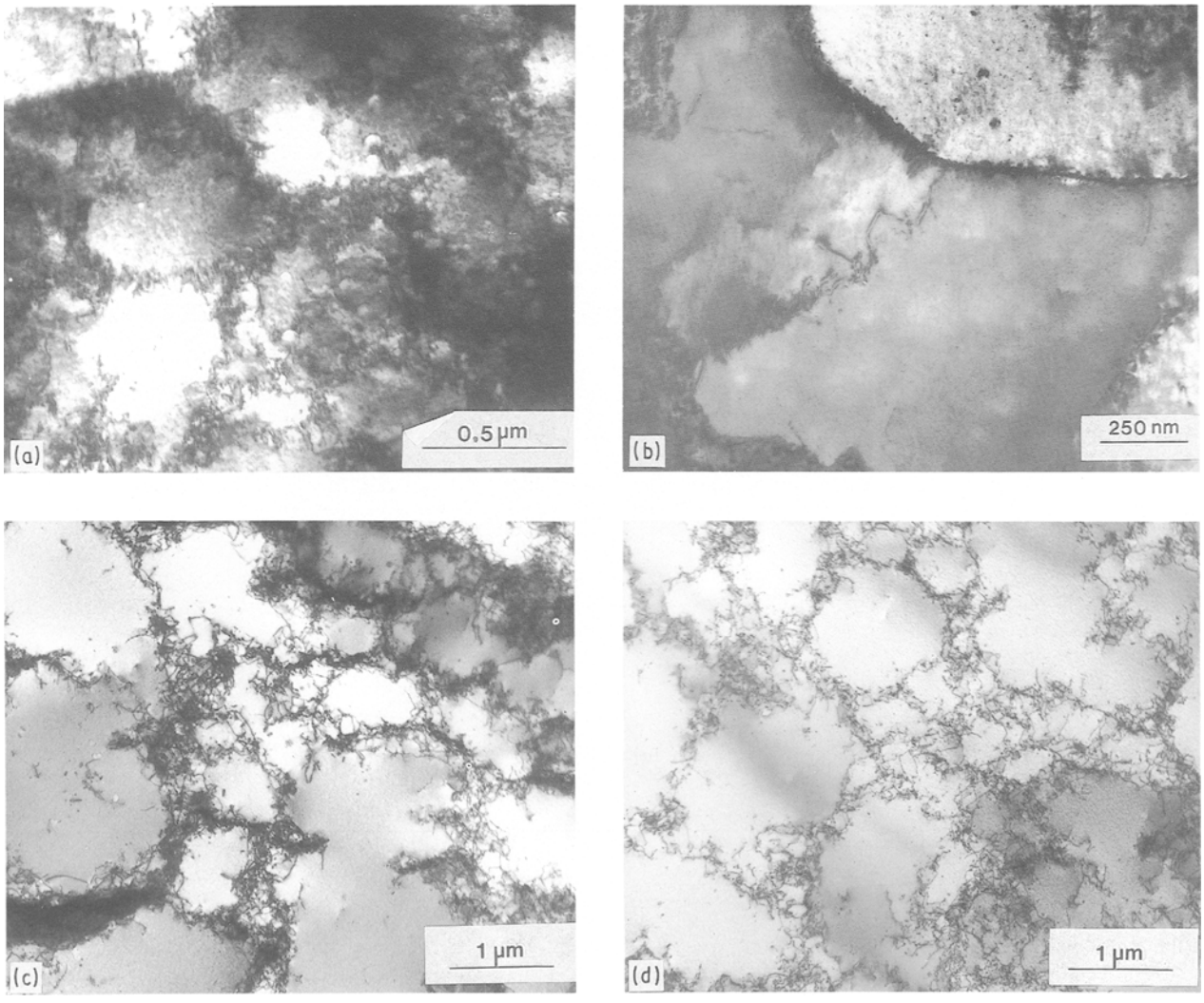

Figure 4 (a–d).

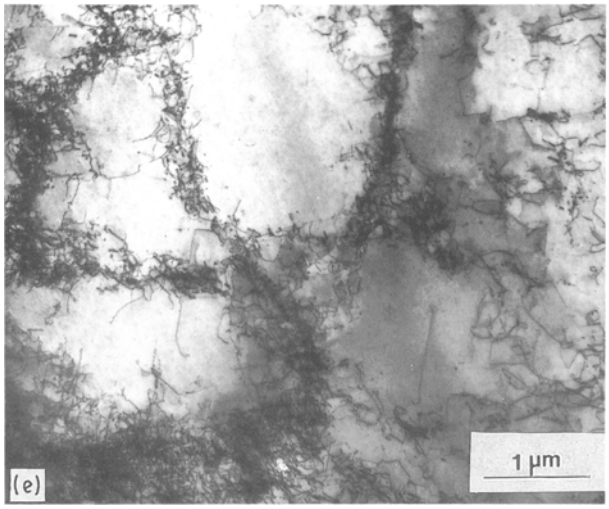

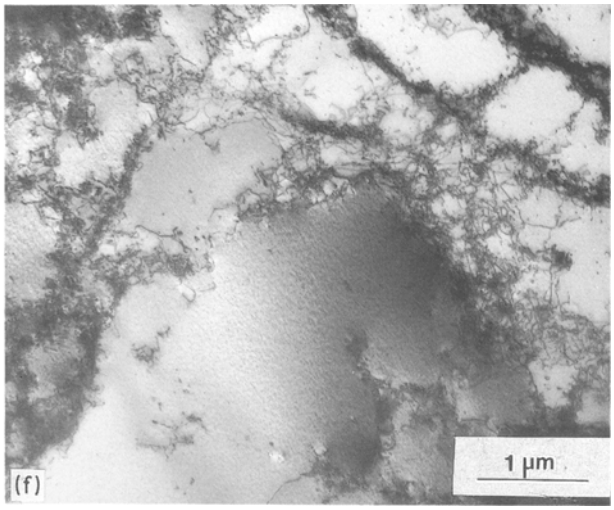

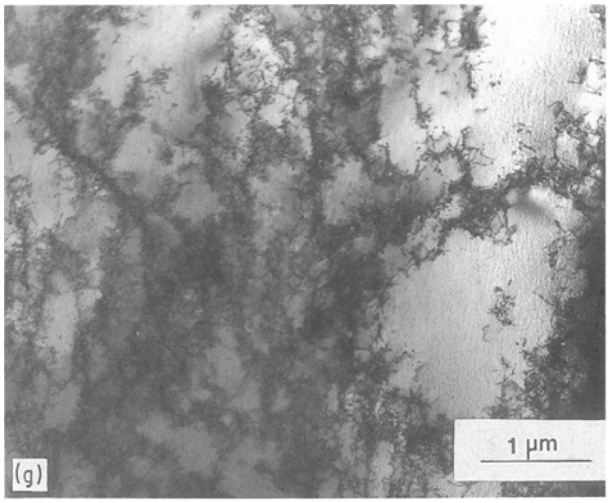

Figure 4 Transmission electron micrographs showing (a) cell structure in cold-worked as-received Ni 270; (b) dislocation-free grains in statically recrystallized nickel at 750 K; (c, d) imperfectly developed subgrain structure in nickel tested at 1100 K, $\varepsilon = 35\%$ at ambient pressure, and (e) at high pressure; (f) non-recovered areas and dislocation-free subgrains in the same creep conditions as above at 1 atmosphere, and (g) high pressure.

of cell sizes (Fig. 4c–e). Although quantitative measurements have not been performed, it appears that the subgrain size is almost similar in 0.1 and 1500 MPa specimens. This observation implies that the peak stress values at these two types of pressure environment are comparable. Unfortunately, an experimental verification of this assumption was not possible. While peak stress values were measured in 1 atm creep experiments, such measurements were not available in the high-pressure tests due to experimental difficulties [1]. Again, at both pressures, free dislocation cells can frequently be seen in the neighbourhood of completely non-recovered area where dislocation tangles are still clearly visible (Fig. 4f and g).

4. Discussion

The recrystallization behaviour of nickel 270 is consistent with literature data. While grain growth followed regular kinetics for 1 atm pressure experiments, it was considerably slower under 1500 MPa pressure. It is clear that in 1 atm experiments, grain growth is controlled by grain-boundary diffusion processes. If the diffusion coefficient is constant at a certain homologous temperature, then pressure application lowers the diffusivity. This decrease is explained by the general increase of the melting point at high pressures. Indeed, as shown in a previous paper [1], the activation energy for grain-boundary diffusion may be expected to increase at high pressures due to preferential volume contraction in regions of less efficient packing. Consequently, high-pressure application retards grain growth, as observed experimentally. In addition, the wavy grain boundaries (Fig. 3b) are further evidence of lower grain-boundary mobility at high pressure.

The oscillations in flow stress and the metallographic observation of recrystallized grains are two strong indications that dynamic recrystallization takes place during 1 atm creep experiments. In addition, the as-observed imperfectly developed dislocation substructure in the recrystallized grain could only be produced by high-temperature deformation after recrystallized grains had formed. Despite the uncertainty in the nickel SFE value [7–11] it is well established that nickel recrystallizes both under creep conditions (i.e. high temperature and low strain rates) and hot working (high temperature and high strain rates) in a similar way as low stacking fault energy metals do. The initial work hardening cannot be removed sufficiently rapidly by polygonization and enough strain energy is available to initiate recrystallization. Recrystallization is initiated every time a critical strain, ε_{cr}, is attained. In constant strain-rate experiments, recrystallization is completed in a time that is characterized by the strain occurring in that time, ε_x. Oscillations are observed when $\varepsilon_x \leqslant \varepsilon_{cr}$ or one recrystallization cycle is complete before the next recrystallization cycle starts. Our experimental oscillation pattern is consistent with Luton and Sellars' theory on dynamic recrystallization in which each oscillation corresponds to a recrystallization cycle [7]. Furthermore, oscillations increase at higher temperatures and lower strain rates in agreement with the above theory because recrystallization is enhanced and ε_x is reduced accordingly, despite the decrease of critical strain at higher temperatures. In contrast, as seen in Fig. 2, at low temperature (1100 K) and low

strain rates ($10^{-3}\,s^{-1}$), oscillations dampen out because a new recrystallization wave is set off before the previous one is completed. As shown by Sandstrom and Lagneborg [12], the onset of dynamic recrystallization is controlled by a critical dislocation density, ρ_{cr}, which is given by the expression

$$\rho_{cr} = \frac{4\sigma_{surf}}{\tau d^*} \quad (2)$$

where σ_{surf} is the grain-boundary energy per unit area, τ is the average energy per unit length of a dislocation, and d^* is the diameter of the recrystallization nucleus. The size of critical nucleus, d^*, is smaller than the grain diameter, probably by a factor of two, but greater than the average subgrain diameter. This critical dislocation density is related to critical strain for recrystallization to be set off by the expression

$$\varepsilon_{cr} = \boldsymbol{b} l_d \rho_{cr} \quad (3)$$

where $\boldsymbol{b}$ is the Burgers vector and l_d is the mean free path of dislocations in the subgrain wall. Therefore, the driving force for recrystallization is essentially supplied by the dislocation energy stored in the subgrains walls. This driving force exists in both 1 atm and high-pressure experiments.

While for 1 atm experiments there is no doubt that oscillations are strictly related to dynamic recrystallization, at high pressure these oscillations are not clearly defined. Nevertheless, the presence of a dislocation substructure in high-pressure specimens is a clear indication that dynamic recrystallization occurs and is controlled by dislocation accumulation due to power-law creep. Moreover, different cell sizes along with dislocation-free and dislocation-filled grains (Fig. 4g) are also indicative of a recrystallization followed by a non-steady on-going deformation–recovery process. Finally, the waviness of a grain boundary may be taken as evidence of strain-induced boundary migration that usually occurs in a recrystallized material only after small or moderate amounts of strain.

Considering that the grain diameter is an upper limit to d^* in Equation 2, the critical dislocation density is significantly larger in high-pressure specimens because their initial grain size is smaller than that in 1 atm specimens. Therefore, the recrystallization frequency is less in high-pressure specimens than in 1 atm specimens in spite of the presence of more recrystallization nuclei. Additionally, at high pressure, the mobility of grain boundaries is significantly inhibited and thus probably results in slow nucleation and grain-growth processes. Indeed, Sandstrom and Lagneborg calculated grain size in dynamically recrystallized nickel based on the assumption that nucleation occurs at mobile grain boundaries [12]. Then the small grain size at high pressure is to be expected because low grain-boundary mobility seriously inhibits dynamic recrystallization and growth.

The restricted accuracy of stress measurements in high-pressure experiments could also account for the lack of clear display of oscillations due to dynamic recrystallization. The change in oscillation patterns with pressure is in agreement with the results of Ghosh and Raj [13], i.e. dynamic recrystallization is more visible when grain size become larger, as in our specimens crept at ambient pressure. In coarse-grained material the power-law creep may cause sufficient accumulation of dislocations to allow the nucleation of new stress-free grains.

The observed lower strain-induced grain growth at high pressure as compared to ambient pressure may also be attributed to significantly lower diffusion rates. At 1 atm, cascade recrystallization at critical strains in increasingly larger grains deformed by recovery-controlled dislocation creep may explain the strain-induced grain growth.

5. Conclusions

1. High-pressure application considerably retards recrystallization and grain-growth kinetics due to an increase in activation energy for grain-boundary diffusion, compared to ambient pressure.

2. Dynamic recrystallization occurs during creep testing in the 0.63–0.9 T_m temperature range and 0.1–1500 MPa pressure range. However, the kinetics of dynamic recrystallization is significantly slower at high pressures. Sandstrom and Lagneborg's theory on dynamic recrystallization correlates well with our experimental results.

3. Strain-induced grain growth was observed during creep in the above-mentioned temperature and pressure ranges.

Acknowledgement

The authors thank the Office of the Basic Energy Sciences, Department of Energy (Grant DE-F603-88ER45360).

References

1. S. MEAGHER, R. S. BORCH, J. GROZA, A. K. MUKHERJEE and H. W. GREEN II, *Acta Metall. Mater.* **40** (1992) 159.
2. J. P. POIRIER, *Acta Metall.* **26** (1978) 629.
3. *Idem, ibid.* **27** (1979) 401.
4. J. WEERTMAN and J. R. WEERTMAN, in "Constitutive Relations and Their Physical Basis", edited by S. J. Andersen, J. B. Bilde-Sorensen, N. Hansen, T. Leffers, H. Lilholt, O. B. Pedersen and B. Ralph (Riso National Lab, Roskilde, Denmark, 1987) p. 191.
5. I. HAESSNER and S. HOFMANN, in "Recrystallization of Metallic Materials", edited by F. Haessner (Riederer, Stuttgart, 1978) p. 76.
6. B. A. PARKER, R. G. O'DONNELL and N. K. PARLE, in "Constitutive Relations and Their Physical Basis", edited by S. I. Andersen, J. B. Bilde-Sorensen, N. Hansen, T. Leffers, H. Lilholt, O. B. Pedersen and B. Ralph (Riso National Lab, Roskilde, 1987) p. 459.
7. M. J. LUTON and C. M. SELLARS, *Acta Metall.* **17** (1969) 1033.
8. C. NORMAN and S. A. DURAN, *ibid.* **18** (1970) 723.
9. D. HARDWICK and W. J. McG. TEGART, *J. Inst. Metals* **90** (1961–62) 17.
10. H. ZHU and S. K. VARMA, *Met. Trans.* **21A** (1990) 500.
11. D. HARWICK, C. M. SELLARS and W. J. McG. TEGART, *J. Inst. Metals* **90** (1961–62) 21.
12. R. SANDSTROM and R. LAGNEBORG, *Acta Metall.* **23** (1975) 387.
13. A. K. GHOSH and R. RAJ, *ibid.* **34** (1986) 447.

Received 7 October
and accepted 27 November 1991